ELSEVIER

Int. J. Therm. Sci. 41 (2002) 115–123

International Journal of Thermal Sciences

Thermal hydraulic characterization of a heat pipe with extracapillary circulation

G. Canti, G.P. Celata *, M. Cumo, M. Furrer

Institute of Thermal–Fluid Dynamics, ENEA Casaccia, Energy Department, Via Anguillarese, 301-00060 S.M. di Galeria, Roma, Italy

Received 16 March 2001; accepted 28 June 2001

Abstract

Heat pipe devices, for their typical working mechanisms, are particularly suitable for zero gravity applications, and have also been considered for applications in space satellites with nuclear propulsors, thanks to the absence of mobile systems for the coolant fluid circulation.

The present work reports the results of experimental tests carried out on a heat pipe facility designed to investigate the thermal–hydraulic performance of a water heat pipe.

The device layout, configuration and geometry, allow to simulate a heat pipe working utilizable in space applications and so under zero gravity conditions. The evaporating section, completely lined by wicks (sintered stainless steel), and nearly plane shaped, is housed in a cylindrical container.

Two test series were performed with reference to different heater sizes (heated plate—wick contact surface size), obtaining for the evaporating heat flux q''_{ev} a value of 13 W·cm^{-2} in the 1st series and of 20 W·cm^{-2} in the 2nd one, using a smaller heater size. This result means a potential possibility to use more compact evaporators and to work at higher system operating pressure values. It was possible to establish the increase of the limit heat flux q''_{evl} versus the operating pressure in a range of 50–400 kPa. The condensate subcooling, due to the subcooler in the external channel, sensibly affects the boiling and the wick dispriming.

In conclusion, it is necessary to point out that the obtained results are only preliminary and relative to a pilot test section. Further tests will be carried out with appropriate changes in the configuration, in the geometry and in the operating conditions.

Keywords: Heat pipe; Zero gravity; Space; Thermal hydraulic performance; Experimental

1. Introduction

Heat pipe devices, for their typical mode of working, are particularly proper for zero gravity applications. They have also been considered for applications in space satellites with nuclear propulsors, thanks to the absence of active systems for the coolant fluid circulation.

Conventional heat pipes are sealed tubes, which transport heat from a heat source to a heat sink using the latent heat of vaporization of a liquid heat carrier (working fluid). The heat is released by condensation at the heat sink and then the condensed liquid is transported back to the evaporator zone by capillary forces. The capillary action is exerted by proper wicks or by proper axial or circumferential grooves, respectively arranged or carved on the tube internal surface.

The capability of heat flux transfer from the evaporator region to the condenser region can be increased by high proper working fluid surface tension and solid surface wettability (wick fluid contact angle) and is instead limited essentially by liquid pressure drop and boiling inside the wick.

The experiments conducted and described in the present work allowed the preliminary evaluation and the characterization of the thermal–fluid dynamic behaviour and related performances of a heat pipe whose layout and configuration devices allow the simulation of the steady-state conditions of hypothetical heat pipes utilizable in 0-g space environment.

* Correspondence and reprints.
E-mail address: celata@casaccia.enea.it (G.P. Celata).

1290-0729/02/$ – see front matter
PII: S1290-0729(01)01289-3

Nomenclature

A_c	condenser internal surface	m^2	
A_{ev}	evaporating zone surface	m^2	
A_v	condenser steam flow passage section	m^2	
ΔH_{ec}	water level	m	
Γ_{ls}	condenser coolant flow rate	$kg{\cdot}s^{-1}$	
l_{ev}	evaporator length	m	
l_g	top-bottom wick level difference	m	
l_l	liquid zone length	m	
p	pressure	Pa	
Q_{el}	electric power	W	
Q_{sc}	thermal power transferred to the condenser coolant	W	
q''_c	heat flux at the condenser	$W{\cdot}m^{-2}$	
q''_{ev}	heat flux generated in the evaporator ..	$W{\cdot}m^{-2}$	
q''_{evl}	limit heat flux generated in the evaporator	$W{\cdot}m^{-2}$	
q''_{tran}	heat flux transferred from the evaporator to the condenser	$W{\cdot}m^{-2}$	
T	temperature	°C	

2. Heat pipe space applications

The heat pipe represented schematically in Fig. 1, typically utilizable in zero gravity environment, consists essentially of the following sections:

(1) the evaporator/heating section completely lined by porous material (wick);
(2) the adiabatic transmission section lined by longitudinal wick sectors which originate free longitudinal channels (arteries), as shown in the particular of Fig. 1;
(3) the condenser section (radiator), partially or completely lined by wicks.

The layout of the wick sectors and the free channels, arteries, in the transmission section is necessary to ensure the start-up of the system and to improve the heat flux transfer in steady-state conditions. Concerning this, it is important to recall the attention to the wick priming problem, indispensable to the capillary action generation.

In a heat pipe working in horizontal position, like that shown in Fig. 2, in the earth ($g \neq 0$), the priming can be ensured by a correct inventory of the working fluid and is sufficient to line by wick only the evaporator. If the heat pipe orientation is slightly inclined and the condenser region is at a lower level than the evaporator one, the initial fluid inventory is able to interest the condenser, then it is necessary to completely line by wicks the heat pipe.

In the space ($g = 0$) if all the heat pipe sections are completely lined by wicks, unfavourable condition which causes too large pressure drop along the length of the heat pipe, it may happen that after a transient acceleration phase from g (earth) to zero (space), during a satellite launch phase, it is not possible to ensure that the fluid will remain confined inside the wick. Instead, it may be that the fluid arrangement occurs in the vapour region with subsequent dispriming of the wick. This last chance is not easy to occur, so in any case even considering that a part of liquid remains confined in the wick region, it is necessary to ensure as much as possible the wick continuity between the evaporator and the condenser, reducing at the same time the wick lining of the internal surface for lowering the pressure drop. For this reason, as shown in Fig. 1, some free channels may be left in the heat pipe transmission region.

In this configuration, it is possible to assume that at the start-up, when the heat flux is low, the wick sectors are primed and so the fluid circulation occurs throughout them. Then, gradually, the fluid accumulates in the free channels, the arteries, and when they are completely filled, flooded from the evaporator to the condenser, then the

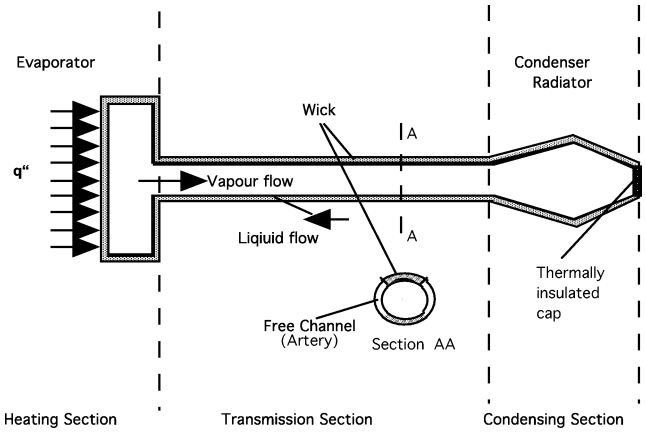

Fig. 1. Schematic of a possible heat pipe for zero gravity application with partial extracapillary circulation.

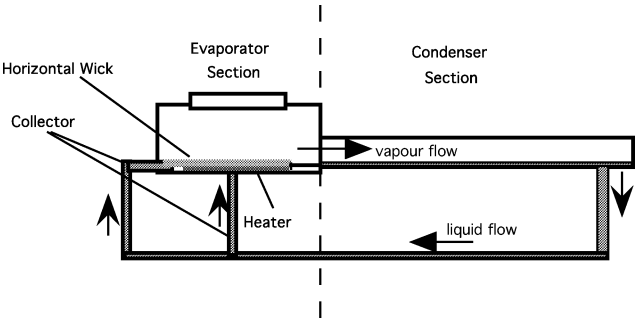

Fig. 2. Schematic of heat pipe working in horizontal position and simulating a zero-gravity situation.

liquid circulation occurs throughout them due to the smaller pressure drop exerted. Under these circumstances of wick external circulation (extracapillary circulation) the heat flux transferred is much larger due to the increase of the liquid and then of vapour flow rate. The system can operate under stable conditions with a sensible increase in performances than the start-up phase.

3. Experimental apparatus and test section design

A complete sketch of the experimental facility, called ETCA, reported in Fig. 3 and schematically shown in Fig. 4, is characterized by an external channel which connects the condenser exit to the collector of the evaporator section. This channel is completely filled by working liquid (water), is not lined by wicks and simulates one of the free channels present in the transmission section of the space heat pipe tube, as represented in Fig. 1. Obviously, in absence of the priming problem and if one could assure that, under transient conditions, gravity/non gravity transition effects, the fluid remains confined in the mentioned external channel and the coolant circulation, or whatever heat sink, remains extended on the bottom condenser region, the ETCA test section configuration would be preferable than that shown in Fig. 1, unless different nature constraint conditions.

The layout of the shaped truncated-cone heated surface and of the wick allows to introduce a conservative gap on test performances. In fact, with g gravity, the generation of a possible and unwanted thermosiphonic circulation in the external loop can be opposed by the gravitational drop due to the wick inclination (cone shaped). It is the case, to point out that horizontal heated surfaces, and relative wicks, simulate very well the gravity absence giving rise to the only pressure drop due mainly to the flow in the internal wick. A vertical position of the heated surface would, instead, cause the flooding of the low region and would prevent the remaining upper region to be wet by liquid.

The lower portion of the evaporator wall is surrounded by an annular collector from which the wick sucks the condensate which is pushed, through a short capillary way, to the upper heated wick zone.

The ETCA test section has been designed for a pressure of 3 bar, corresponding to a water saturation temperature of 135 °C. The steam chamber is equipped with an observation window 150 mm in diameter and 20 mm in thickness. The heated wall, with a surface of 100–150 cm^2, is very close to the window and is lined by a truncated-cone shaped wick which transports the condensate drawn in the annular collector located at a lower level.

The wick consists of a sintered stainless steel plate 3 mm in thickness and 90 μm in porosity, modelled just to perfectly adhere to the heater wall. A dense number of holes, 3 mm in

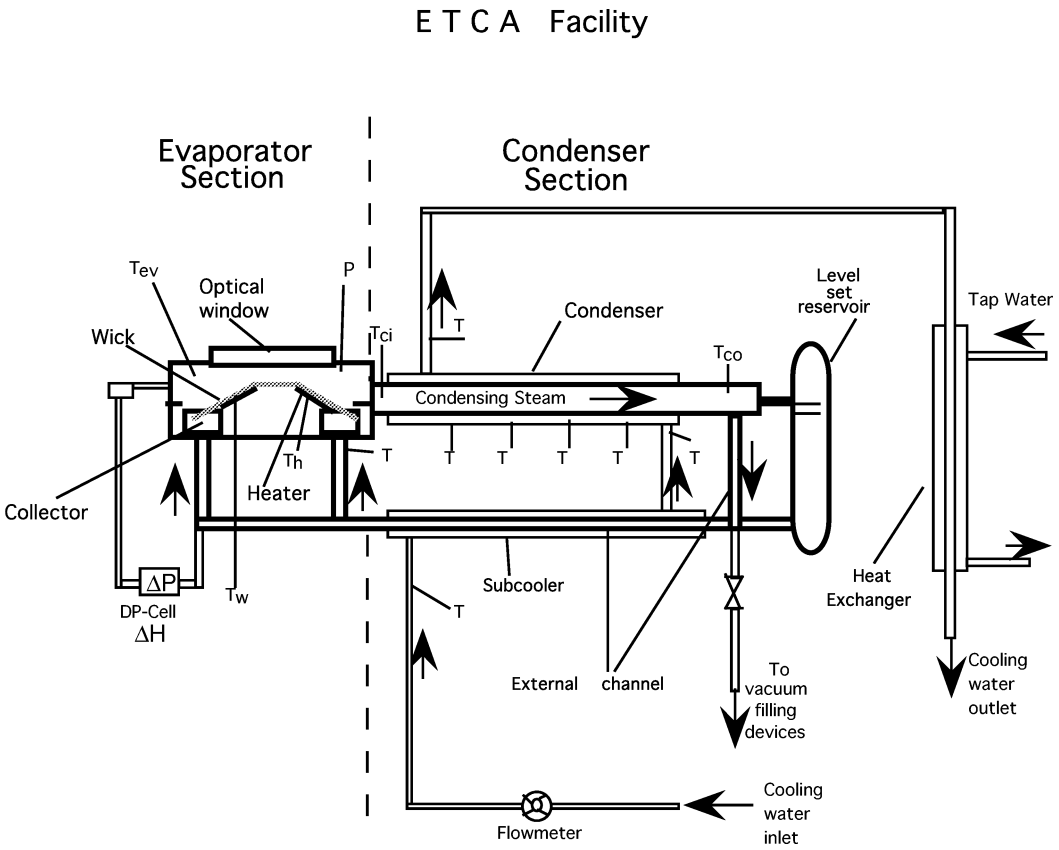

Fig. 3. Sketch of the ETCA experimental facility.

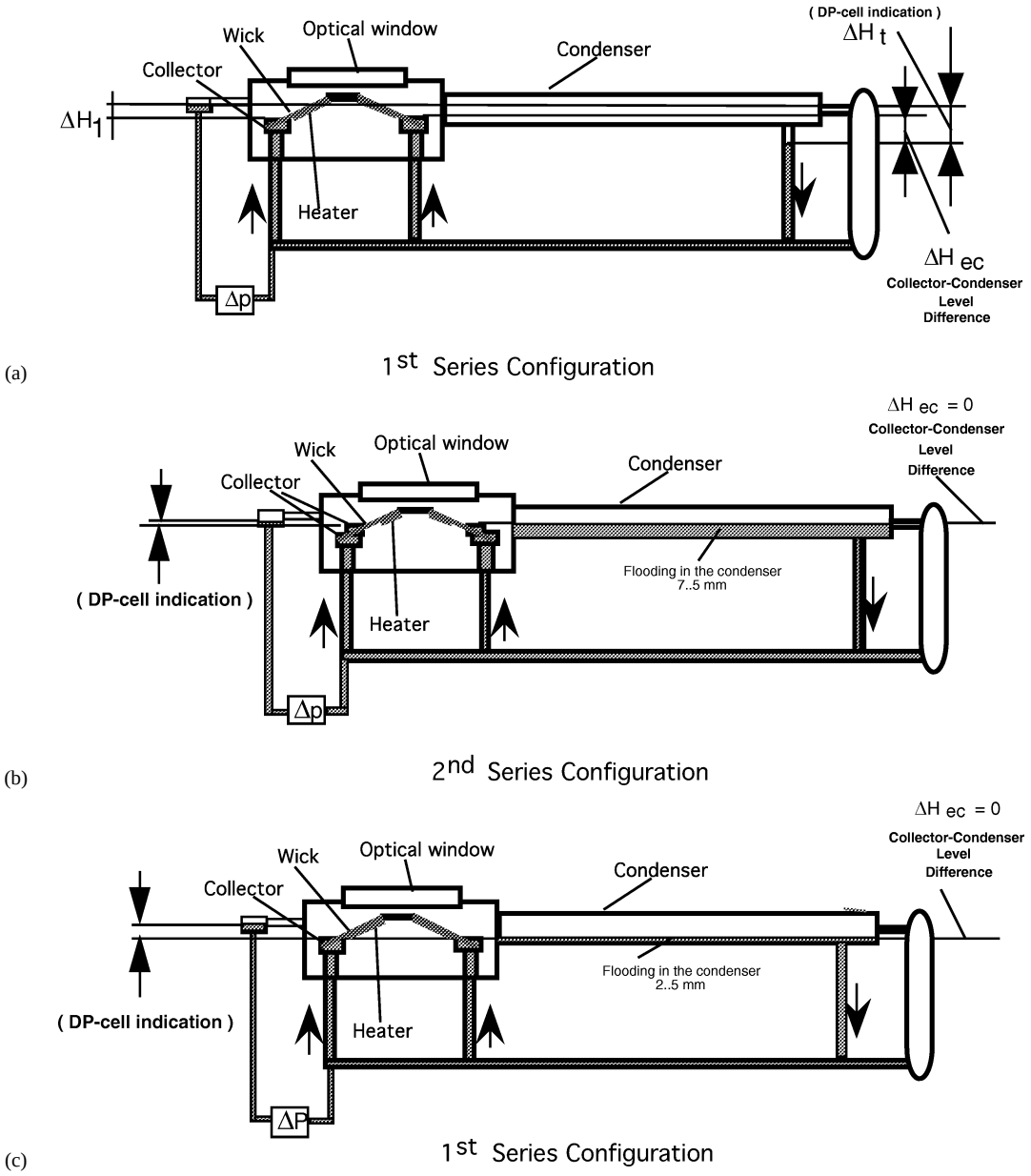

Fig. 4. Schematic of the test section, concerning level difference set-up for the two test series.

diameter, opportunely disposed, aids the exit of the steam generated in the wall-wick interstice.

In this experimental phase, the transmission section is absent in the ETCA configuration. So, the steam coming from the evaporator section flows directly in the condenser inlet section. The condenser coolant water, i.e., the cold sink of the heat pipe, flows in an external annular channel and its controlling flow-rate, Γ_{ls}, allows to change the condenser thermal conductance and so, for a fixed heat load, the ETCA operating pressure. In the annular section a spiral wire has been wrapped on the internal tube, just to increase the turbulence and then the heat transfer coefficient.

In the present configuration, the condenser internal surface is not lined with wicks, but it is possible to line partially or completely this surface in which 4 slots are made to locate thermocouples with the aim of evaluating the condensation rate of the incoming steam.

4. Test performance and results

The ETCA facility, shown in Fig. 3, has been used to evaluate thermal-fluid dynamic performances of the ETCA test section, which simulates the operation of a heat pipe for space applications. The first experimental campaign has been carried out, as previously mentioned, without wicks on the condenser section internal surface.

The capillary action, to draw and circulate the working fluid, is exerted by the only portion of wick present in the evaporator section and the condensate returning flow

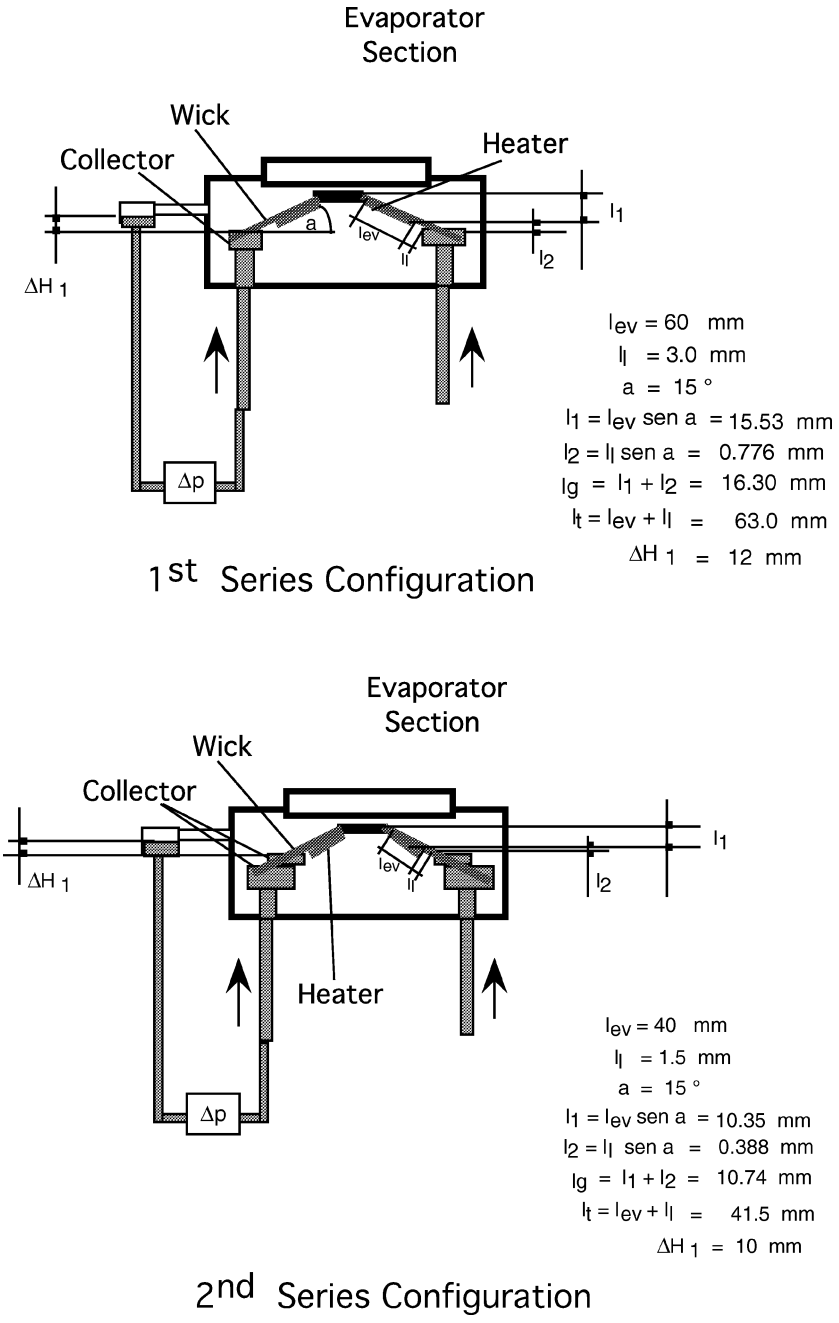

Fig. 5. Evaporator configuration for the two test series.

comes throughout an external channel (an artery, as an extracapillary circulation) which includes the subcooler. This heat exchanger, subcooling the condensate, allows to operate with a higher heat flux because the consequent lower collector inlet fluid temperature opposes an eventual wick dispriming due to steam bubbles generation and transport in the collector region which feeds the wick. The data acquisition was referred to steady-state operating conditions of the system.

To evidence the evaporating zone length effect l_{ev}, two series of tests were carried out with reference to two different geometrical configurations of the wick and of the heated region. Figs. 4 and 5 show the geometrical parameters and the layout of the wick and of the heated region for these two configurations which essentially differ for the l_{ev} value. Construction requirements, due to the changes produced to transform the first configuration in the second one, caused also different values for the liquid zone length l_l and for the collector water level (collector upper surface). This latter value is larger in the second configuration, as shown in Fig. 5, in which it is also possible to note that to reduce l_{ev} to 40 mm, it was necessary to decrease the heater external diameter.

The heater located between the wick supported plate and the lower counter-plate was therefore reduced in size thickening the coils towards the inside evaporator region obtaining in this way an evaporating zone surface A_{ev}, (heated plate-wick contact area), of 100 cm^2 against the value of 150 cm^2 of the first series.

The lower value, 1.5 mm, of l_l length, imposed by the constructive changes and used in the 2nd series, compared to 3 mm of the 1st series, even decreasing the wick pressure drop, can produce a more probable dispriming due to steam bubbles formation and transport in the liquid feeding region of the wick. In fact, as shown in Fig. 5, the 1.5 mm l_l value causes a tighter approach of the collector liquid surface to the heated region of the evaporator.

Tests were performed for three initial values of the liquid level difference ΔH_{ec} between the filled collector liquid level (upper surface level) and the vertical tube liquid level of the external channel, artery (Fig. 4(a)). Initial values of ΔH_{ec} affect the gravitational head which otherwise would be due only to the wick inclination and so to l_g value (Fig. 5). The value of ΔH_{ec} was deduced by a DP-cell indication (ΔH_t) under steady-state and cold conditions, and without fluid circulation.

Before any beginning of a daily tests series, vacuum operation with noncondensables extraction was made, followed by wick priming obtained flooding the system with working fluid and then discharging the liquid, through the relative line, to establish the desired initial value of ΔH_{ec}. It is pointed out that the discharge produces a gradual reduction of the system liquid level, until it reaches the collector upper surface level. At this point, the further discharge reduces the level only in the external channel vertical pipe and the collector remains completely filled of liquid, thanks to the depression generated by the wick capillary action.

Furthermore, it is necessary to note that the initial measurement of ΔH_{ec} value is affected by some uncertainties due to the physical conditions existing in the system during level set-up, which is performed at low pressure (corresponding to the vacuum value reached). For this reason, a slight difference in the absolute pressure can cause sensible changes in the noncondensables specific volume with the subsequent possible presence of variable gas volume accumulated in the annular collector and consequent changes in the levels.

Graphs of Fig. 6 show the more significant first series results referred to the heat flux generated in the evaporator and transferred to the condenser:

$$q''_{ev} = Q_{sc}/A_{ev} \tag{1}$$

and to the condenser heat flux:

$$q''_{c} = Q_{sc}/A_{c} \tag{2}$$

in which:

Q_{sc} power transferred to the condenser coolant;
A_{ev} heated plate-wick contact surface;
A_c condenser internal surface;

as a function of the difference between the wall and the steam saturation temperature. The heat flux is observed to be a strong, increasing function of the operating pressure.

Graphs of Fig. 7 show q''_{ev} values versus difference between the wall and the steam saturation temperature in the second series, for a pressure range of 50–400 kPa (top graph), and for three ΔH_{ec} values (0.5, 1.0 and 2.0 cm water column) (bottom graph), where the heat flux generated in the evaporator, as already shown in Fig. 6, increases as $T_w - T_s$ increases.

The graph of Fig. 8 shows a comparison between the two test series in terms of q''_{ev}, evidencing the expected and higher 2nd series q''_{ev} heat flux values up to 20 W·cm^{-2}, against 1st series 12–13 W·cm^{-2} maximum values. The difference is due to the sensible reduction of the evaporating surface A_{ev} which, in turn, gives rise to an increase of the wall temperature.

Fig. 9 reports q''_{ev} versus the heater electric power Q_{el} for the two test series. The results plotted in Figs. 8 and 9 allow

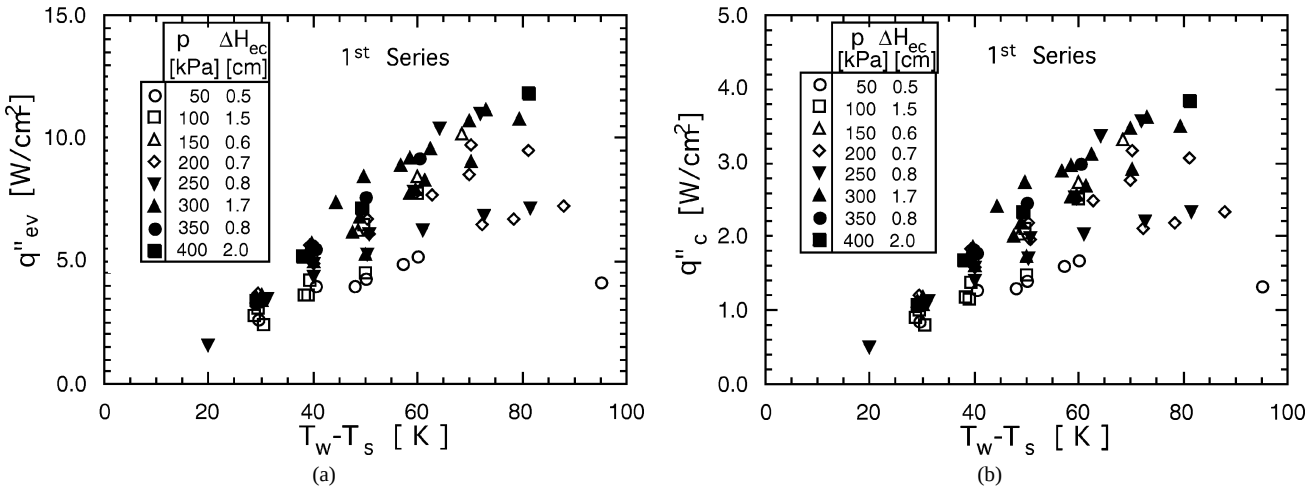

Fig. 6. Heat flux generated in the evaporator (a) and transferred from the condenser (b) versus wall to saturated steam temperature difference (1st test series).

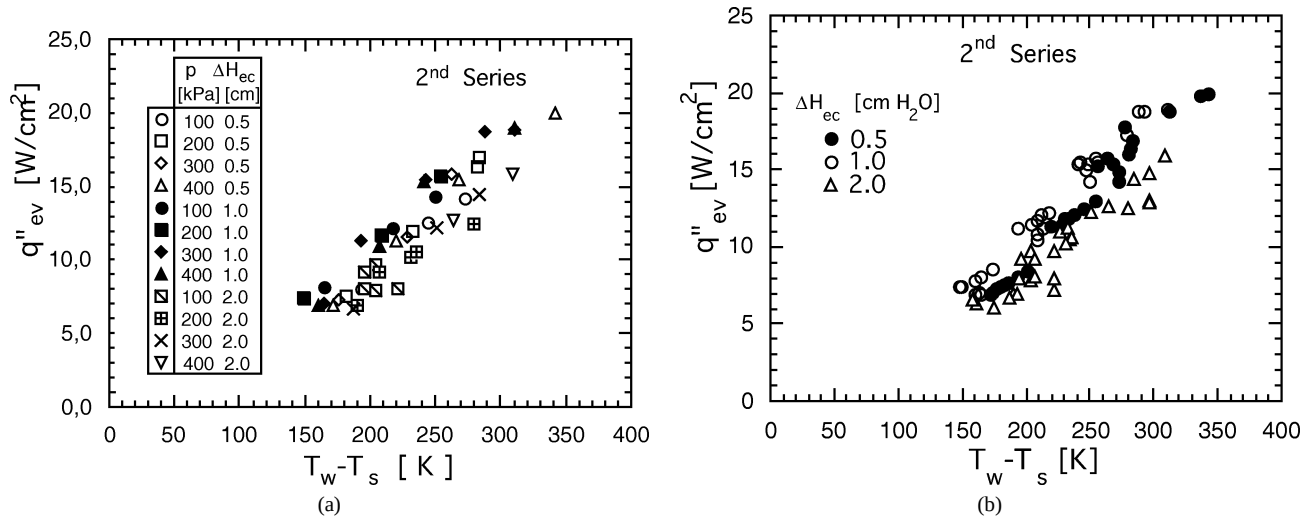

Fig. 7. Heat flux generated in the evaporator versus wall to saturated steam temperature difference (2nd test series), evidencing pressure and level dependence (a) and level dependence (b).

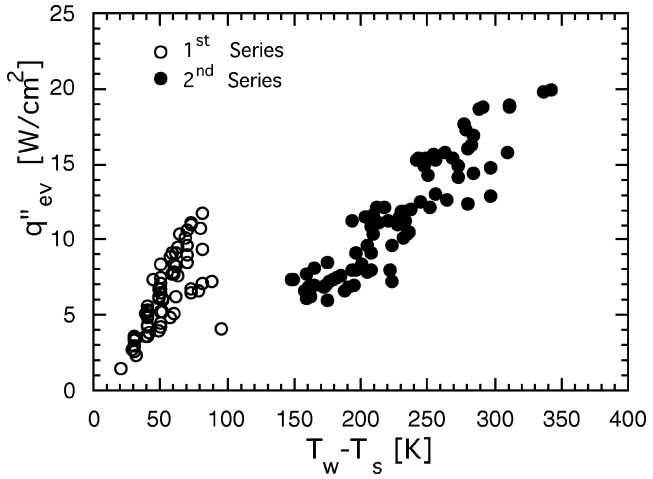

Fig. 8. Global comparison of the heat flux generated in the evaporator for the two test series versus wall to saturated steam temperature difference.

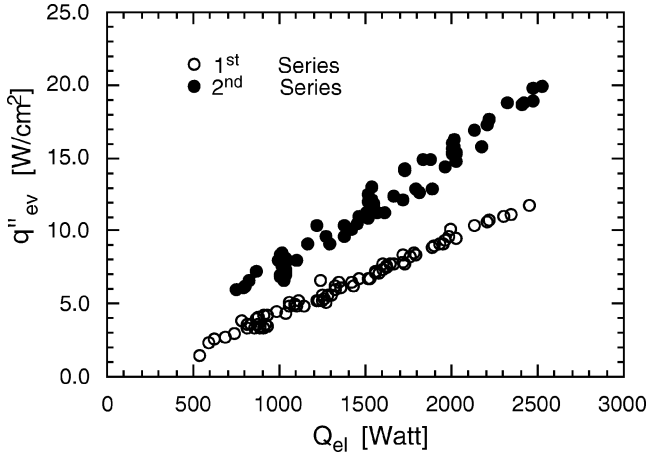

Fig. 9. Global comparison of the heat flux generated in the evaporator for the two test series versus the electric power delivered to the heater.

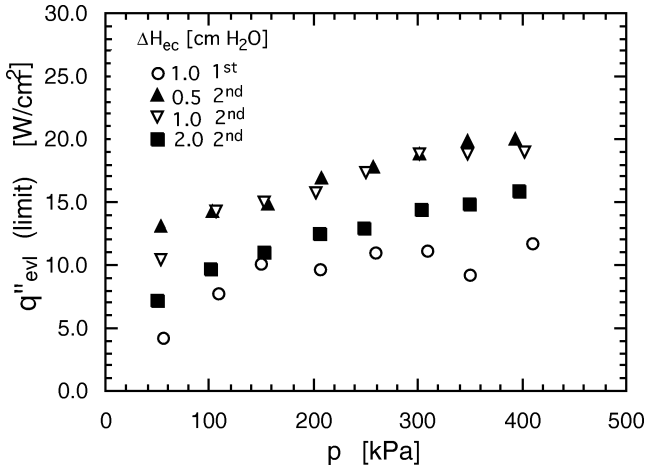

Fig. 10. Heat flux limit versus pressure for the two test series.

to claim that is possible to reduce the evaporator size, thus increasing q''_{ev}, accepting the consequent wall temperature increase.

The graph of Fig. 10, where the heat flux limit value q''_{evl} is plotted versus the operating pressure p, evidences as q''_{evl} depends on the ETCA system operating pressure. The heat flux limit is due to the dispriming for receding liquid or to the boiling limitation.

Referring to the second series, the graph shows a q''_{evl} value of 13 W·cm^{-2} and 20 W·cm^{-2} for a pressure of 50 kPa and 400 kPa, respectively. In the graph of Fig. 11 are reported q''_{ev} values both in limit and normal operating conditions versus pressure and for fixed electric power Q_{el}. It is possible also to note in this graph that for a fixed Q_{el} value and for normal operating condition (non limit), q''_{ev} value is nearly independent of the pressure.

For what concerns the steam transferred from the evaporator to the condenser, i.e., the heat flux $q''_{tran} = Q_{sc}/A_v$, in which A_v is the condenser steam flow passage section, it is

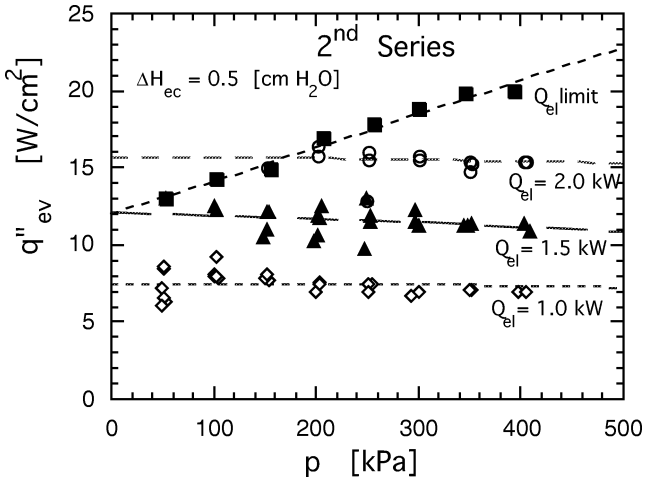

Fig. 11. Heat flux generated in the evaporator versus pressure and for a fixed heater electric power: limit and normal operating conditions values (2nd test series).

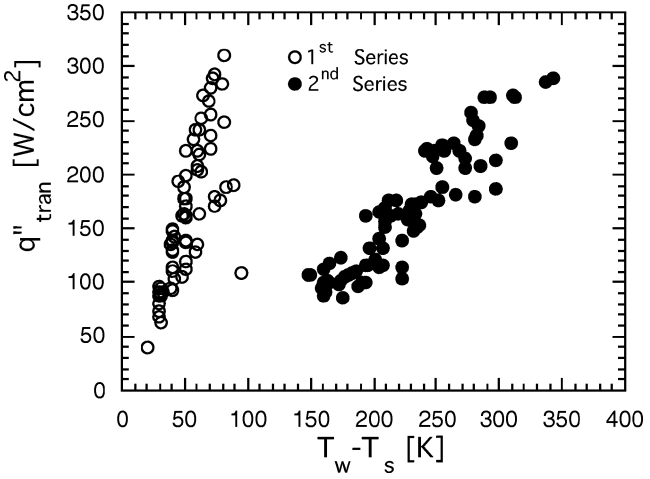

Fig. 12. Heat flux transferred to the condenser versus wall to saturated steam temperature difference for the two test series.

possible to verify on the graph of Fig. 12, as q''_{tran} values are almost the same in the two configurations, although there is a sensible evaporator wall temperature increase due to the decreasing of the contact surface A_{ev}. In fact, even if different values exist between the two configurations (l_{ev}, l_{l}, l_{g}, the wick cross-sectional area along the cone line, the condenser inlet section, the initial condenser flooding), the possibility to change the thermal conductance of the heat pipe system acting on the condenser coolant flow rate Γ_{ls}, allows the system to operate at the same pressure values. More exactly, working at the same electric power Q_{el} in the two series, it is possible to operate at different flow rate Γ_{ls}, but such to establish equal pressure values and therefore equal Q_{sc} and, for the same A_{v}, to obtain equal q''_{tran} values.

In the graph of Fig. 7 it appears that, in non limit operating conditions, for $\Delta H_{\text{ec}} = 1.0$ cm, even if the gravitational head is larger than that relative to the test with $\Delta H_{\text{ec}} = 0.5$ cm, the heat flux q''_{ev} is greater. The reason can be due to the test parameter imperfect reproducibility, that suggests a further, more accurate verification.

5. Conclusions

The results obtained in the two test series allowed first to confirm some indications already found in preliminary tests performed using simple devices simulating a portion of the ETCA evaporating section (wick-heater-collector) [16].

First of all it was confirmed that the heat flux q''_{ev} increases with the heater diameter reduction (heated plate-wick contact surface), i.e., the evaporating zone length l_{ev}, obtaining a value of 20 W·cm^{-2} with l_{ev} equal to 40 mm in the 2nd series and a value of 12 W·cm^{-2} with l_{ev} equal to 60 mm in the 1st series (Fig. 8). This result means a potential possibility to use a more compact evaporator and to work with a higher system operating pressure.

It was possible to establish the increase of the limit heat flux q''_{evl} (Fig. 10) with the operating pressure in a range of 50–400 kPa.

The condensate subcooling, due to the subcooler in the external channel, sensibly affects the boiling and the wick dispriming. Saturation conditions in the collector zone close to the heater, detected by a proper thermocouple, cause in fact bubble generation and consequently possible wick dispriming. For these reasons it is necessary a more suitable heater location and thermal insulation with respect to the collector.

The higher collector liquid level in the 2nd configuration (Fig. 4) and the unaltered wick size, implies that the wick has a larger portion submerged in the collector and, consequently, in a more subcooled zone (due to the greater distance from the heater). This fact guarantees a more probable preservation and/or priming recovery consequent to the eventual upper zone dispriming.

Finally, it is pointed out that under operating conditions with partial wick flooding (determined by a fluid level higher than the collector superior surface level), the system performances are reduced due to partial liquid stagnation in the collector zone near to the wick and to the heater. In fact, in this case the evaporating liquid is in part fed (replaced) by that which is superior to the wick self, and so the circulation rate is reduced and a probable boiling can occur. Under zero gravity conditions, an eventual liquid excess would not cause necessarily a falling on the wick self.

References

[1] K. Cornwell, B.G. Nair, Boiling in wicks, Proc. Heat Pipe Forum Meeting, Publ. as National Engineering Laboratory, Report N. 607, 1976.
[2] Heat Pipes-properties of common small-pore wicks, Data Items N. 79013, Engineering Sciences Data Unit, London, 1979.
[3] R.A. Moss, A.J. Kelley, Neutron radiographic study of limiting heat pipe performance, Internat. J. Heat Mass Transfer 13 (3) (1970) 491–502.

[4] J.K. Ferrell, R. Davis, H. Winston, Vaporization heat transfer in heat pipe wick materials, in: Proc. 1st Internat. Heat Pipe Conference, Stuttgart, October 1973.

[5] W.R. Davis, J.K. Ferrell, Evaporative heat transfer of liquid potassium in porous media, in: AIAA/ASME Thermophysics and Heat Transfer Conference, Boston, MA, July 1974.

[6] E.G. Alexandra, Structure property relationship in heat pipe wicking materials, Ph.D. Thesis, N.C. State University, 1972.

[7] P.D. Dunn, D.A. Reay, Heat Pipes, 4th edn., Pergamon Press, 1994.

[8] D. Keser, Experimental determination of properties of saturated sintered wicks, in: Proc. 1st Internat. Heat Pipe Conference, Stuttgart, October 1973.

[9] H.M. Winston, J.K. Ferrell, R. Davis, The mechanism of heat transfer in the zone of the heat pipe, Proc. 2nd Internat. Heat Pipe Conference, Bologna, 1976, ESA SP-112, Vol. I.

[10] G.F. Smirnov, B.A. Afanasiev, Investigation of vaporization in screen-wick-capillary structures, in: Proc. 4th Internat. Heat Pipe Conference, London, Advances in Heat Pipe Technology, Pergamon Press, 1981.

[11] M.D. Xin, H.D. Xie, Y.G. Chen, Boiling heat transfer on heating surfaces covered by metal screens, in: Proc. 5th Internat. Heat Pipe Conference, Tsukuba, 1984.

[12] T.Z. Ma, Z.F. Zhang, H.Q. Li, Vaporization heat transfer in capillary wick structures formed by sintered screens, in: Proc. 5th Internat. Heat Pipe Conference, Tsukuba, 1984.

[13] C.Y.L. Chan, C. Sall, Capillary head and permeability of wicks with single or multiple size pores, in: Proc. 8th Internat. Heat Pipe Conference, Beijing, 1992.

[14] H. Kozai, H. Imura, K. Takashima, Effective thermal conductivity of screen wicks, in: Proc. 3rd Internat. Heat Pipe Symposium, Tsukuba, 1989.

[15] W.S. Chang, Porosity and effective thermal conductivity of wire screens, J. Heat Transfer 12 (1990) 5–9.

[16] G. Canti, G.P. Celata, M. Cumo, M. Furrer, Thermal hydraulic characterization of stainless steel wicks for heat pipe applications, Rev. Gen. Thermique 37 (1) (1998) 5–16.